



Short communication

Identification of aplysinopsin as a blood-brain barrier permeable scaffold for anti-cholinesterase and anti-BACE-1 activity

Vijay K. Nuthakki^{a,b,1}, Rammohan R. Yadav Bheemanaboina^{a,b,1}, Sandip B. Bharate^{a,b,*}

^a Medicinal Chemistry Division, CSIR-Indian Institute of Integrative Medicine, Canal Road, Jammu 180001, India

^b Academy of Scientific & Innovative Research, Ghaziabad 201002, India



ARTICLE INFO

Keywords:

Aplysinopsin
Acetylcholinesterase
Butyrylcholinesterase
BACE-1
N-sulphonamide
Molecular modeling
BBB permeability
Alzheimer's disease

ABSTRACT

Aplysinopsins are a group of marine-derived indole alkaloids that display diverse array of pharmacological effects. However, their effect on anti-Alzheimer targets has not been reported. Herein, we report the synthesis of aplysinopsin (**1**) and its effect on cholinesterases and beta-site amyloid-precursor protein cleaving enzyme 1 (BACE-1). It inhibits electric eel acetylcholinesterase (AChE), equine serum butyrylcholinesterase (BChE), and human BACE-1 with IC₅₀ values of 33.9, 30.3, and 33.7 μM, respectively, and excellent BBB permeability (P_e 8.92 × 10⁻⁶ cm/s). To optimize its sub-micromolar activity, the first-generation analogs were prepared and screened. Two most active analogs **5b** and (Z)-**8g** were found to effectively permeate the BBB (P_e > 5 × 10⁻⁶ cm/s). The N-sulphonamide derivative **5b** display better cholinesterase inhibition, whereas the other analog (Z)-**8g** strongly inhibits BACE-1 (IC₅₀ 0.78 μM) activity. The analog **5b** interacts primarily with PAS of AChE, and thus exhibit a mixed-type of inhibition. In addition, aplysinopsin along with new analogs inhibited the self-induced Aβ₁₋₄₂ aggregation. The data presented herein indicate that the aplysinopsin-scaffold holds a potential for further investigation as a multi-targeted anti-Alzheimer agent.

1. Introduction

Alzheimer's disease (AD) is a complex multi-faceted neurodegenerative disease which is the significant health-care challenge in 21st century [1]. Fervent research has led researchers to identify diverse range of potential targets; however, not much is known about the actual cause of AD, and no curative treatments are available to date [2–4]. The amyloid-β (Aβ) is a major hallmark in AD pathology, which comprises a sequential cleavage of amyloid precursor protein (APP) by β- and γ-secretases followed by oligomerization, and fibrillation [4]. Several studies have shown therapeutic relevance of beta-site APP cleaving enzyme 1 (BACE-1, β-secretase) in AD [5,6]. Thus, it has emerged as a clinically validated target for AD [7,8]. Furthermore, numerous studies [9–14] have shown that butyrylcholinesterase (BChE) also plays a vital role in the progression of AD along with acetylcholinesterase (AChE). Thus, targeting both AChE and BChE appears to be a more viable approach to combat AD. As a whole, all available knowledge and research efforts made in this area are indicative of the fact that multi-targeted approaches (agents able to engage more than one target) have a great future to tackle AD [15]. Given this, recently, we screened a

library of ~100 small molecule natural products against three targets (AChE, BChE, BACE-1) and identified embelin as a multi-targeted anti-Alzheimer agent [16]. From this screen, aplysinopsin (**1**) was one of the active showing significant inhibition of all three enzymes AChE, BChE, and BACE-1, along with excellent blood-brain barrier (BBB) permeability.

Historically, marine organisms have proved to be an extremely valuable source of lead candidates and drugs [17]. Aplysinopsins is one of the important class of marine sponge-derived indole alkaloids [18–28] that are known to possess diverse array of biological activities [19,21,29–31]. Aplysinopsin (**1**) also modulate monoamine oxidase, nitric oxide synthase, and serotonin receptors [32]; however, is not yet been tested against cholinesterases or BACE-1. In the present communication, we report the discovery of aplysinopsin (**1**) as a new scaffold for cholinesterase and BACE-1 inhibition with an ability to cross the BBB.

* Corresponding author at: Medicinal Chemistry Division, CSIR-Indian Institute of Integrative Medicine, Canal Road, Jammu 180001, India.

E-mail address: sbharate@iiim.res.in (S.B. Bharate).

¹ V.K. Nuthakki and R.R.Y. Bheemanaboina, contributed equally as a first author.

2. Results and discussion

2.1. Identification of aplysinopsin as a dual cholinesterase/BACE-1 inhibitor

Aplysinopsin was synthesized in two steps starting from commercially available creatinine (**9**). The first step involves methylation of creatinine (**9**) using iodomethane [**33**]. The *N*-methyl creatinine (**10**) was then condensed with indole-3-carboxaldehyde (**11**) to get aplysinopsin (**1**) (Fig. 1A). The synthesized aplysinopsin (**1**) was a part of our internal natural product (NP) collection, which was utilized for searching multi-targeted NP scaffolds that can cross BBB. In this anti-Alzheimer drug discovery campaign [16,34,35], the screening of internal collection of small molecule NPs in cholinesterase and BACE-1 inhibition assays have provided 'aplysinopsin' as active NP against all three targets (Fig. 1B) along with an added advantage of its excellent BBB permeability ($P_e = 8.92 \times 10^{-6}$ cm/s). The molecular docking has shown that aplysinopsin (**1**) occupies the active-site gorge of both AChE and BChE, showing interactions with residues of catalytic anionic site (CAS) as well as peripheral anionic site (PAS). Its imidazolidin-4-one ring display π - π stacking with Trp 86 of anionic subsite of AChE. The NH of imidazolidin-4-one ring have shown H-bonding interaction with carbonyl oxygen of His 447 of CAS, whereas the carbonyl oxygen of imidazolidin-4-one ring display H-bonding with Phe 295 of acyl binding pocket. The indole ring interacts with Trp 286 and Tyr 341 residues of PAS via π - π stacking. In BChE active site gorge, aplysinopsin oriented in a similar direction, with imidazolidin-4-one ring facing towards CAS. In the BACE-1 active site, though it displayed π - π stacking and H-bonding interactions with some of the active site residues; however, the interaction with a catalytic dyad (Asp 32, Asp 228) was missing which perhaps explains its weak BACE-1 inhibition activity (Fig. 1E).

2.2. Synthesis of aplysinopsin analogs

To improve the activity profile of aplysinopsin, its first-generation derivatives/analogues were synthesized. Aplysinopsin (**1**) is a small molecule comprising two key functionalities viz. indole and imidazolidinone. To prepare first-generation analogues with improved anti-cholinesterase and/or anti-BACE-1 activity, we planned two set of

simple modifications viz. the introduction of sulphonamide moiety on indole ring and replacing the indole with other aryl units. Verubecestat is a sulphonamide class of BACE-1 inhibitor that was investigated in phase III clinical trial in AD [36]; thus it was hypothesized that sulphonamide derivatives will enhance the BACE-1 inhibition. Secondly to know the necessity of indole moiety as a part of pharmacophore for observed anti-cholinesterase or anti-BACE-1 activity, it was decided to replace it with simple substituted aryls.

The sulphonamide derivatives **5a-5c** were prepared by reacting aplysinopsin (**1**) with different substituted sulphonyl chlorides **6a-6c** in the presence of 4-dimethylaminopyridine (DMAP) and *N,N*-diisopropylethylamine (DIPEA) (Fig. 2A). Next, we replaced the indole ring of aplysinopsin with different substituted aryl/heteroaryls. The treatment of various aryl/heteroaryl aldehydes **7a-7i** with *N*-methyl creatinine (**3**), yielded a pair of *E*- and *Z*- isomers of **8a-8i**, as shown in Fig. 2B. Using this scheme, a library of 19 aplysinopsin analogs were synthesized. In all cases, except naphthyl aldehydes and 2,4-dichlorobenzaldehyde, we observed the formation of creatinine-linked pair of isomers. The assignment of the respective isomers was done using 2D-NMR experiments such as nuclear overhauser effect spectroscopy (NOESY) and heteronuclear multiple bond correlation (HMBC). Furthermore, the ^1H NMR of a pair of isomers displayed a unique trend for the chemical shift value of C7-H proton. This trend was well in correlation with the TLC retention factor of these isomers.

The isomers that elutes slow on TLC (e.g. **8a (L)**, $R_f = 0.35$) were found to show slightly low chemical shift value (δ 5.98 ppm) for C7-H proton compared with other isomer (e.g. **8a (U)**, $R_f = 0.43$). This trend was common among all six pairs that we investigated and is presented in Table 1. The proper assignment of these isomers was done by performing NOESY experiment (Fig. 3) for one pair of isomers (*E*)-**8g** and (*Z*)-**8g**. The NOESY spectrum of the isomer that eluted first on TLC [upper spot: **8g-(U)**] displayed a contour for NOE between hydrogen of the double bond (C7-H) and the 2'-methyl group of the imidazolinone ring (N2'-Me) which confirmed its geometrical configuration as *E*-isomer i.e. (*E*)-**8g**. In the case of other isomer [lower spot on the TLC: **8g-(L)**], the absence of contour in the NOESY spectrum for N2'-Me and C7-H (Fig. 3B) confirmed its geometrical configuration as *Z*-isomer i.e. (*Z*)-**8g**. Thus, based on the NOESY correlations and the ^1H NMR/TLC observations, the generalization can be done for this class of compounds that *E*-

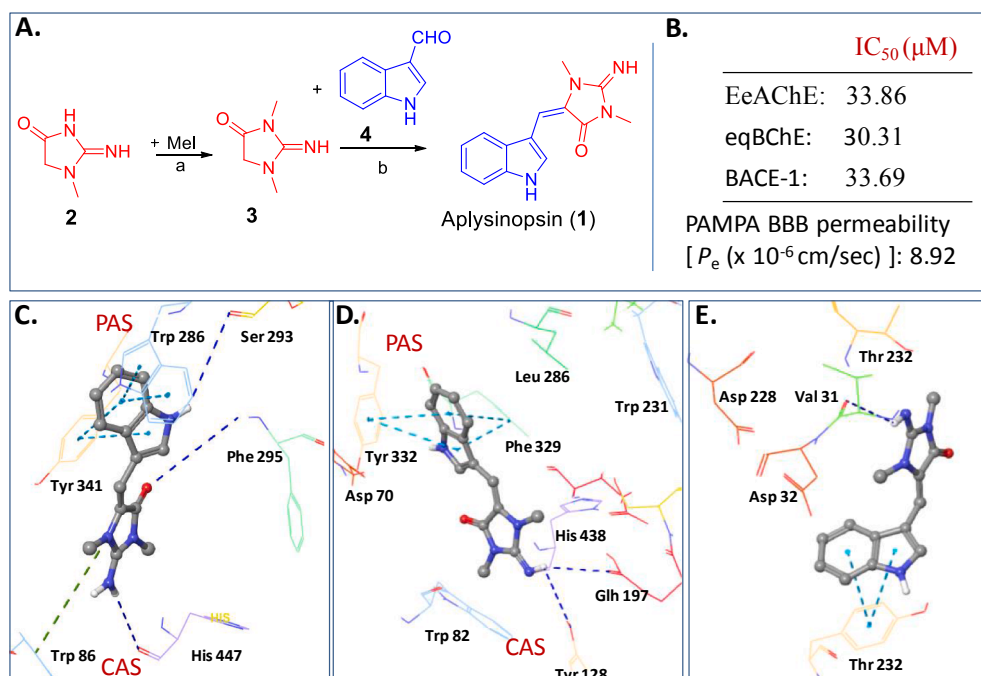


Fig. 1. Identification of aplysinopsin (**1**) as an anti-Alzheimer agent. (A). Synthetic scheme for aplysinopsin synthesis. Reagents and conditions: (a) EtOH, 80 °C, overnight; (b) Piperidine, AcOH, reflux, overnight; (B) AChE, BChE and BACE-1 inhibitory activity and BBB permeability data for aplysinopsin; (C). Interactions of aplysinopsin with AChE (PDB: 4EY7); (D). Interactions of aplysinopsin with BChE (PDB: 6EP4); (E). Interactions of aplysinopsin with BACE-1 (PDB: 4B05). Abbreviations: EeAChE: electric eel AChE; eqBChE: equine serum butyrylcholinesterase; BACE-1: beta-site APP cleaving enzyme 1.

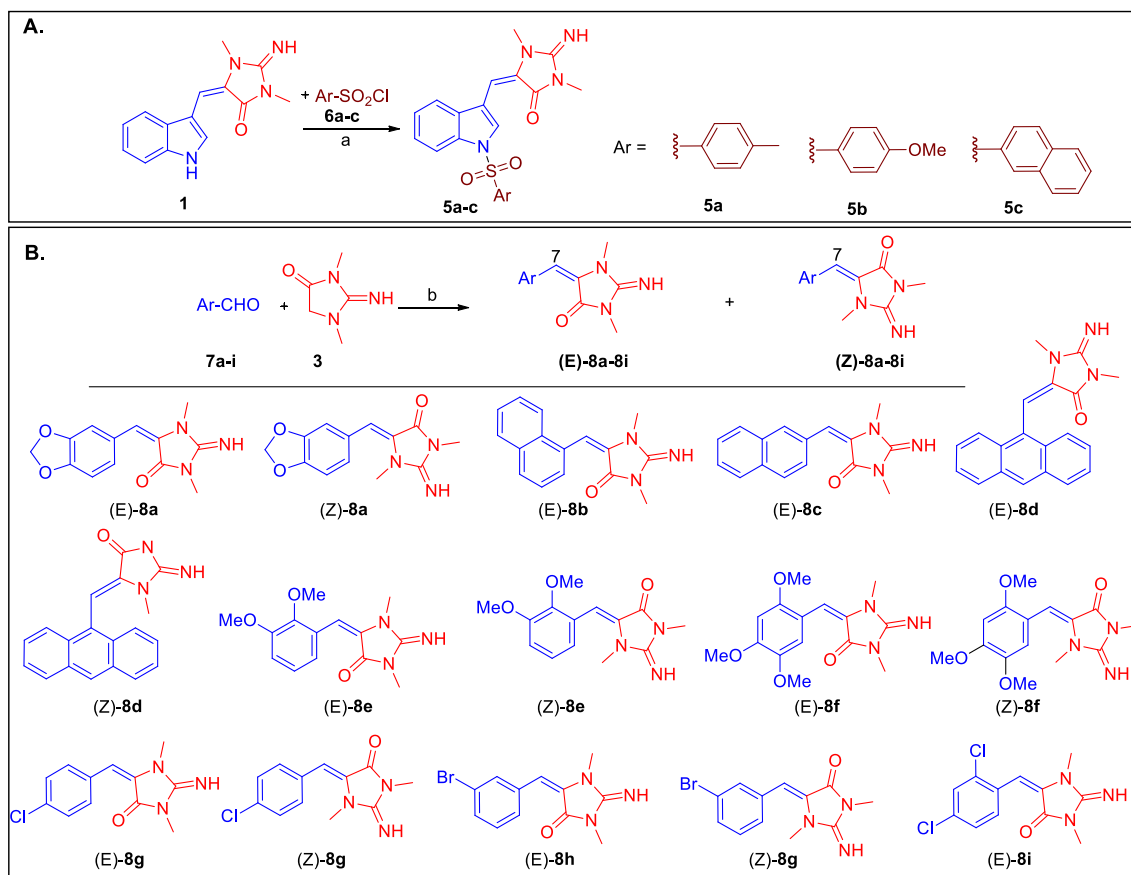


Fig. 2. Synthesis of aplysinopsin analogs: (A). Synthesis of sulphonyl derivatives **5a-5c**. Reagents and conditions: (a) ArSO_2Cl **6a-6c** (1.1 equiv.), DMAP (0.05 equiv.), DIPEA (1.5 equiv.), methylene chloride, room temperature, 20 h. (B). Synthesis of aplysinopsin analogs **8a-8i**. Reagents and conditions: (b) piperidine, AcOH, reflux, overnight. Only one isomer formed for **8b**, **8c**, and **8i**.

isomer elutes slow on TLC than Z-isomer. This generalization will help in the characterization of all such isomers synthesized in the future, only based on the TLC R_f and ^1H NMR patterns.

Table 1

Comparison of E- and Z-isomers in their proton NMR shift and thin-layer chromatography (TLC) retention factor (R_f) values.

Entry		E/Z	Double bonded proton (C7-H) [δ in ppm]	TLC R_f
1 ^a	8a (L) ^c	E	5.98	0.35
	8a (U)	Z	5.99	0.43
2 ^b	8d (L)	E	6.82	0.56
	8d (U)	Z	7.52	0.62
3 ^b	8e (L)	E	6.57	0.38
	8e (U)	Z	6.78	0.45
4 ^b	8f (L)	E	6.49	0.22
	8f (U)	Z	6.52	0.31
5 ^b	8g (L)	E	6.15	0.52
	8g (U)	Z	6.86	0.59
6 ^b	8h (L)	E	6.13	0.61
	8h (U)	Z	6.84	0.67

^a TLC mobile phase: 50% Ethyl acetate/hexane.

^b TLC mobile phase: 30% Ethyl acetate/hexane.

^c Letters L and U mentioned in the parentheses next to the compound numbers indicate the lower and upper spot of TLC isolated from the pair of E- and Z-isomers.

2.3. In-vitro screening of aplysinopsin analogs for cholinesterase and BACE-1 inhibition

All synthesized compounds were screened for inhibition of BACE-1, AChE, and BChE using FRET and Ellman assay (Fig. 4) [37]. It was interesting to note that several compounds have displayed superior inhibition of BACE-1 compared with aplysinopsin (**1**). Compounds **(E)-8g** and **(Z)-8g** were the most active BACE-1 inhibitors showing 47 and 69% inhibition of BACE-1 at 10 μM . For cholinesterase inhibition, the sulphonamide series was most active, with the derivative **5b** showing 60 and 38% inhibition of AChE and BChE, respectively. One of the sulphonamide derivative **5c** inhibited (53, 27, and 41%) all three enzymes.

Next, the IC_{50} values of most active compounds against these enzymes were determined (Table 2). The sulphonamide derivative **5b** inhibited AChE and BChE with IC_{50} values of 3.9 and 14 μM , respectively. Compound **5b** also displayed inhibition of rHuAChE with an IC_{50} value of 21.1 μM . Interestingly, the 4-chlorophenyl analog of aplysinopsin **(Z)-8g** has shown potent inhibition of BACE-1 with IC_{50} value of 0.78 μM . From the obtained results, when compared with the parent compound aplysinopsin (**1**), compounds **(Z)-8g** and **5b** have displayed promising inhibitory potential against BACE-1 and cholinesterases, respectively. Nevertheless, the sulphonamide derivative **5c** exhibited inhibition of all three enzymes (IC_{50} values of 4.9, 19.3, 12.2 μM) with superior potency over aplysinopsin.

2.4. Sulphonamide analog 5b preferentially binds at PAS of cholinesterases

The kinetic analysis of sulphonamide derivative **5b** for recombinant

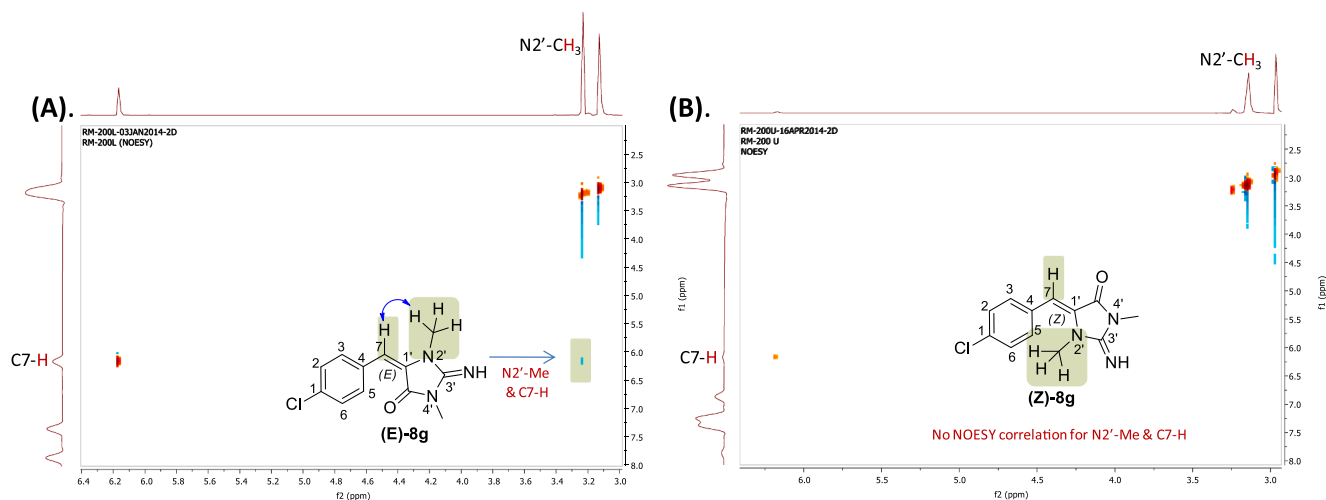


Fig. 3. NOESY correlations for E and Z-isomers of **8g**. (A). NOESY correlation of (E)-**8g** showing the contour for N2'-Me and C7-H indicating the NOE between the hydrogen of the double bond and the N2'-methyl group of the imidazolinone ring. (B). NOESY correlation of (Z)-**8g** in which there is no NOE between the hydrogen of the double bond and the N2'-methyl group of the imidazolinone ring.

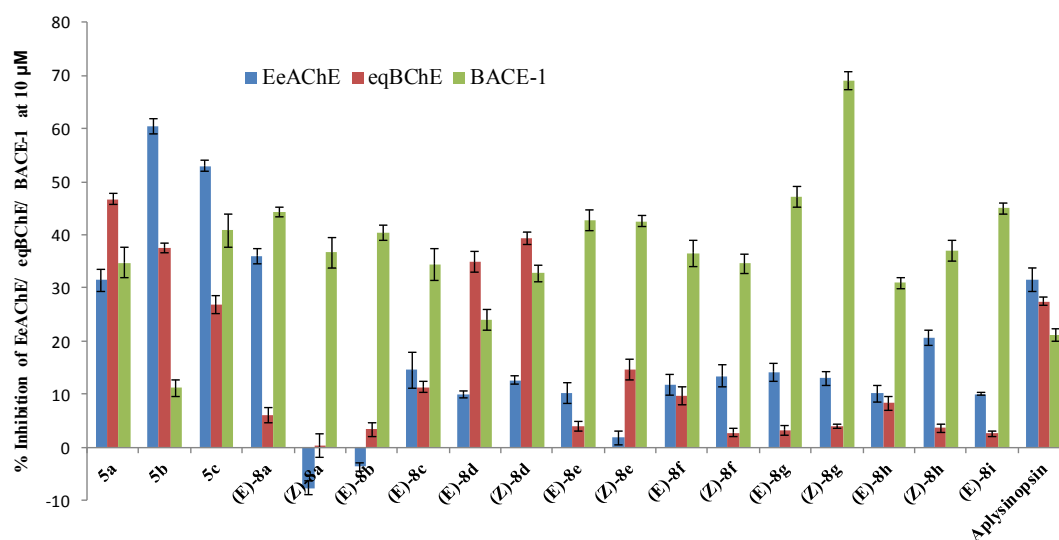


Fig. 4. *In-vitro* inhibition of AChE, BChE, and BACE-1 by natural product aplysinopsin (**1**) along with all synthesized compounds **5a-5c**, **8a-8i** at 10 μM . The percentage inhibition values of AChE, BChE, and BACE-1 are represented as mean \pm SD of three independent experiments. Donepezil and BACE-1 inhibitor IV (Calbiochem IV) were used as positive controls.

human AChE (rHuAChE) and eqBChE inhibition was performed. From Lineweaver–Burk (LB) double-reciprocal plots (Fig. 5A and 5B), the type of inhibition displayed by **5b** was found to be mixed-type for both AChE and BChE, with k_i values of 15.1 and 12.31 μM , respectively. The

Table 2

IC₅₀ values for inhibition of cholinesterases and BACE-1 by selected compounds.

Entry	IC ₅₀ (μM) SD ^a		
	AChE	BChE	BACE-1
1	33.9 \pm 1.67	30.3 \pm 1.31	33.7 \pm 0.90
5a	25.5 \pm 2.24	10.8 \pm 1.16	nd
5b	3.9 \pm 0.73	14.0 \pm 0.45	nd ^b
5c	4.9 \pm 0.68	19.3 \pm 0.88	12.2 \pm 0.34
(Z)- 8g	na	na	0.78 \pm 0.04
Donepezil	0.049 \pm 0.001	5.52 \pm 1.05	nd
BACE-1 inhibitor IV	nd	nd	0.018 \pm 0.001

^a The IC₅₀ values represents the 50% inhibitory concentration of respective enzyme (mean \pm SD of three experiments). nd: not determined; na: not active.

^b **5b** displayed 12% inhibition of BACE-1 at 10 μM .

molecular modeling studies have shown that the sulphonamide **5b** occupies the active-site gorge of AChE; and primarily interacting with PAS (Fig. 5C). The indole ring show π - π stacking with Trp 286/Tyr 341 residues and aryl-sulphonyl ring with Tyr 341 of PAS. Unlike aplysinopsin, the imidazolidin-4-one ring of **5b** oriented towards the mouth of active site gorge (i.e. in the reverse direction), showing H-bonding with Ser 293 residue. In case of BChE, the **5b** oriented in opposite direction as the imidazolidin-4-one ring was found facing towards CAS. The NH of imidazolidin-4-one was found to display a network of H-bonding interactions with Gly 78, Tyr 440, Asp 70 and Tyr 332 residues. The central indole ring show π - π stacking with Tyr 332 residue, and sulphonyl oxygen display H-bonding with Ser 72 residue (Fig. 5D). The preferential interaction with PAS of cholinesterases supported the observed mixed-type inhibition in kinetic study. Further, to support these findings, the affinity of **5b** for the PAS binding site was assessed by displacement of propidium iodide, an AChE ligand that binds explicitly at its PAS binding site. Propidium iodide enhances its fluorescence intensity up to eightfold after binding to AChE [38]. Therefore, the decrease in fluorescence intensity is taken as a measure of displacement

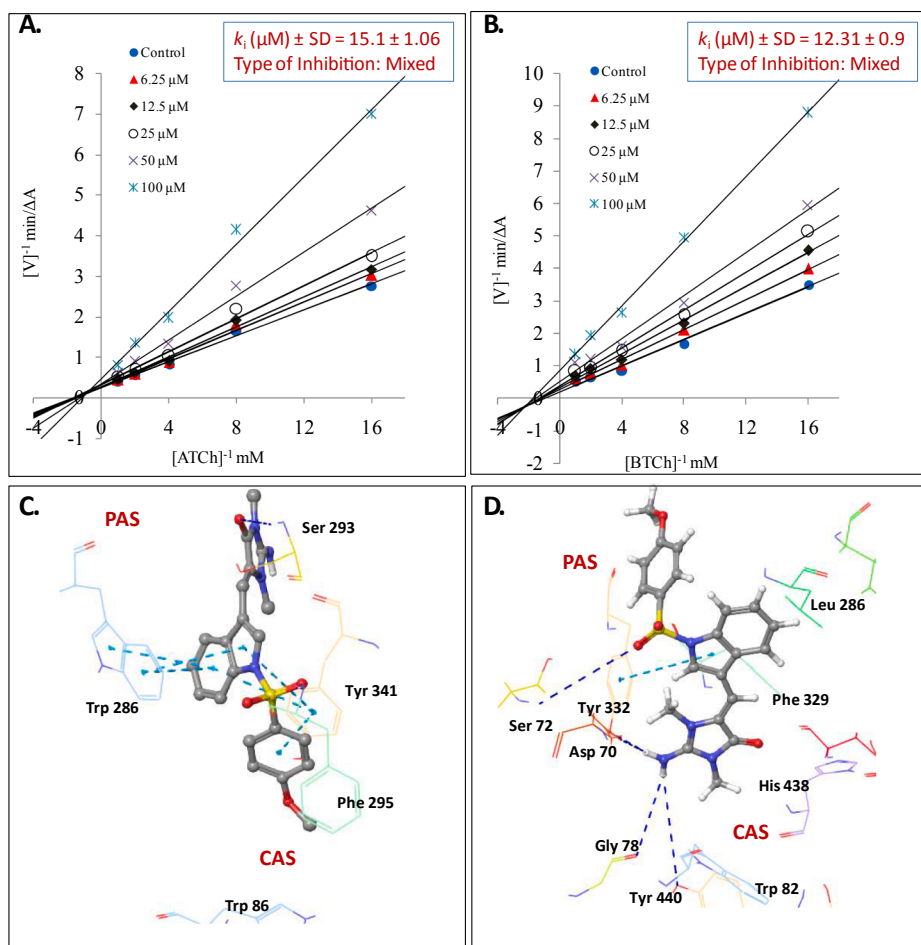


Fig. 5. The kinetics of AChE and BChE inhibition by sulphonamide derivative **5b** and docking studies. (A) The LB plot representing reciprocal of AChE velocity versus reciprocal of different substrate concentrations (0.0625–1 mM) at five different concentrations of **5b**. (B) The LB plot representing reciprocal of BChE velocity versus reciprocal of different substrate concentrations (0.0625–1 mM) at five different concentrations of **5b**. (C) Interactions of aplysinopsin derivative **5b** in the active site gorge of AChE; (D) Interactions of aplysinopsin derivative **5b** in the active site gorge of BChE.

of propidium iodide by compound and affinity of the compound for PAS. Compound **5b** displayed propidium iodide displacement by 26% and 36% at 10, and 50 μM , respectively. This was found to be higher as compared to donepezil, which has shown 21% and 29% displacement at 10 and 50 μM , respectively. These results supported the molecular modeling studies i.e. interactions of **5b** with the residues of PAS binding site. In parallel artificial membrane permeability assay for blood brain barrier (PAMPA-BBB), the analog **5b** was found to be the CNS permeable ($P_e = 5.6 \times 10^{-6}$ cm/s).

2.5. Analog (Z)-**8g** strongly inhibits BACE-1 via mixed-type inhibition

The Lineweaver–Burk double-reciprocal plot (Fig. 6A) has indicated the mode of inhibition for (Z)-**8g** as mixed-type with inhibition rate constant (k_i) of 1.14 μM . In docking studies, the chloro-phenyl ring has shown a range of vital interactions at the active site of BACE-1 (Fig. 6B). The most striking difference between the interaction pattern of aplysinopsin and analog (Z)-**8g** was that the interaction of (Z)-**8g** with the catalytic dyad Asp 32 and Asp 228, which is very important for BACE-1 activity. This interaction was missing in the case of aplysinopsin. In

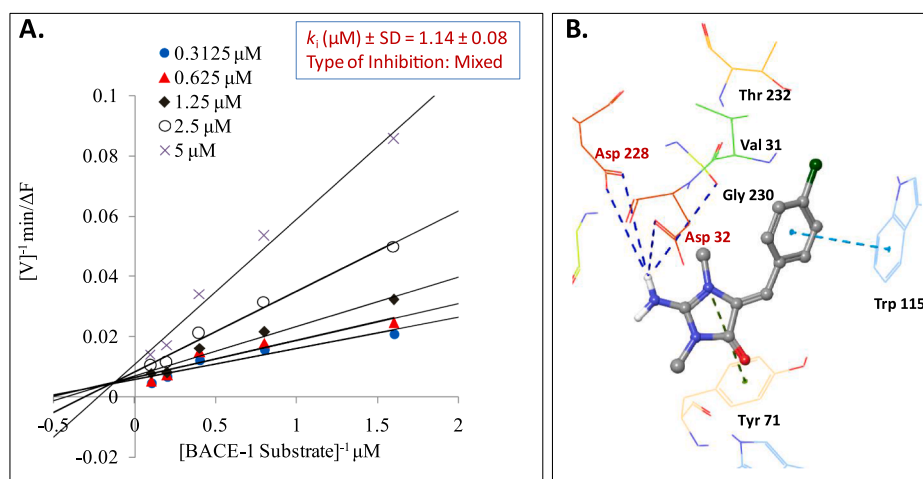


Fig. 6. The kinetics of BACE-1 inhibition by analog (Z)-**8g** and docking studies. (A) The LB plot representing reciprocal of BACE-1 velocity versus reciprocal of different substrate concentrations (0.625–10 μM) at five different concentrations of (Z)-**8g**. (B) Interactions of aplysinopsin analog (Z)-**8g** in the active site of BACE-1. Dark blue, light blue and green dotted lines indicated H-bonding, π - π bonding and cation- π interactions, respectively. (For interpretation of the references to colour in this figure legend, the reader is referred to the web version of this article.)

PAMPA-BBB assay, the analog (Z)-**8g** was found to be CNS permeable ($P_e = 5.3 \times 10^{-6}$ cm/s).

2.6. Aplysinopsin as well as two new analogs **5c** and (Z)-**8g** inhibit the A β 42 aggregation

The inhibitory activity of aplysinopsin (**1**), sulfonamide analog **5b** and 4-chlorophenyl analog (Z)-**8g** against the spontaneous aggregation of A β 42 at 10 μ M was determined in vitro using thioflavin T based fluorometric assay [39]. Curcumin was used as a reference compound in the assay which displayed 70% inhibition at 10 μ M. Test compounds have also significantly inhibited the aggregation of A β with % inhibition values of 69.1, 94.4 and 69.8, respectively for **1**, **5c** and (Z)-**8g**. The analog **5c** which inhibits AChE, BChE as well as BACE-1 was found to be a potent inhibitor of A β 42 aggregation displaying better activity than aplysinopsin and curcumin.

3. Conclusion

In summary, we have identified aplysinopsin (**1**) as a new CNS permeable scaffold for dual inhibition of cholinesterase and BACE-1 inhibition. Aplysinopsin is reported to possess monoamine oxidase (MAO) inhibitory activity (IC_{50} of 5.6 nM) [40,41], and here we found its effect on cholinesterases and BACE-1; thus, this scaffold has multi-targeted activities related to AD. The aplysinopsin derivative **5b** is a dual inhibitor of AChE and BChE (IC_{50} values of 3.9 and 14 μ M), a mild inhibitor of BACE-1, and has excellent BBB permeability. Another sulphonamide derivative **5c** was also able to inhibit all three enzymes AChE, BChE, and BACE-1 with IC_{50} values of 4.9, 19.3, and 12.2 μ M, respectively. The 4-chlorophenyl analog (Z)-**8g** is a potent BACE-1 inhibitor (IC_{50} 0.78 μ M) with excellent BBB permeability. Both **5c** and (Z)-**8g** also inhibited the aggregation of amyloid- β , indicating their potential for further exploration.

The introduction of sulphonamide moiety to the aplysinopsin structure has improved the activity against all three targets (AChE, BChE and BACE-1); however, replacement of the indole ring of aplysinopsin with simple aryl ring e.g. (Z)-**8g** has resulted in loss of anti-cholinesterase inhibitory activity, though it has shown potent inhibition of BACE-1. Thus, for identifying a multi-targeted lead from this scaffold, the indole ring appears to be important, and therefore future lead optimization should be targeted at imidazolidinone core.

4. Experimental section

4.1. General

The chemicals, reagents, glassware, plasticware used in the study were obtained from local suppliers. NMR spectra were recorded on Bruker-Avance DPX FT-NMR 400 MHz instrument. IR spectra were recorded on Perkin-Elmer IR spectrophotometer. HR-ESIMS spectra were obtained from Agilent HR-ESIMS-6540-UHD machine. The enzymes [EeAChE, EC 3.1.1.7; eqBChE, E.C. 3.1.1.8; rHuAChE EC 3.1.1.7], BACE-1 FRET assay kit, other reagents [acetylthiocholine iodide, S-butylthiocholine iodide, Ellman reagent], positive controls [donepezil, β -secretase inhibitor IV] used in biological assays were purchased from Sigma-Aldrich. Absorbance and fluorescence readings were recorded on Molecular Devices, and Biotage microplate readers, respectively.

4.2. Synthesis of 2-imino-1,3-dimethylimidazolidin-4-one (**3**) [33]

Creatinine (**2**, 1 equiv.) and iodomethane (1.2 equiv.) were dissolved in 10 ml of ethanol, and the solution was heated at reflux for 3 h. The progress of the reaction was monitored by TLC. Solvent was removed from the reaction mixture to get titled product **3** as light brown solid.

2-Imino-1,3-dimethylimidazolidin-4-one (**3**). Yield: 78%; light brown

solid; m.p. 210–212 °C; 1H NMR (CD_3OD , 400 MHz): δ 4.27 (s, 2H), 3.21 (s, 3H), 3.18 (s, 3H); ^{13}C NMR (CD_3OD , 100 MHz): δ 170.58, 160.04, 54.54, 32.31, 26.61; IR ($CHCl_3$): ν_{max} 3440, 2922, 2852, 1695, 1633, 1554, 1382, 1261, 1020 cm^{-1} ; HR-ESIMS: m/z 128.0836 calcd for $C_5H_9N_3O + H^+$ (128.0818).

4.3. General procedure for synthesis of aplysinopsin (**1**) and its analogs **8a-8i**

A mixture of the aryl/heteroaryl aldehyde (**4**, **7a-7i**, 1 equiv.), 2-imino-1,3-dimethylimidazolidin-4-one (**3**, 1.1 equiv.) and piperidine (0.5 ml) was stirred in acetic acid (5 ml) at reflux temperature (120 °C) for 8–12 h. The progress of the reaction was monitored by TLC. The reaction mixture was cooled to room temperature, water (10 ml) was added, and the mixture was basified with saturated $NaHCO_3$ solution followed by stirring for 10 min. The precipitate thus obtained was filtered and was finally dried to afford the crude product. This was purified by column chromatography (silica gel #100–200, dichloromethane, and methanol – 99:1–97:3) to get aplysinopsin (**1**) using dichloromethane and methanol (99:1–97:3) and to get analogs **8a-8i** using ethyl acetate and hexane (5:95–50:50) as eluent.

(E)-5-((1H-Indol-3-yl)methylene)-2-imino-1,3-dimethylimidazolidin-4-one (**1**). Yield: 47%; pale yellow solid; m.p. 122–124 °C; HPLC purity: 99% ($t_R = 9.44$ min); 1H NMR ($DMSO-d_6$, 400 MHz): δ 12.05 (s, 1H), 9.29 (s, 1H), 8.98 (d, 1H, $J = 2.8$ Hz), 8.07 (d, 1H, $J = 6.8$ Hz), 7.53–7.51 (m, 1H), 7.30 (s, 1H), 7.27–7.20 (m, 2H), 3.50 (s, 3H), 3.21 (s, 3H); ^{13}C NMR ($DMSO-d_6$, 100 MHz): δ 160.16, 151.83, 135.78, 131.06, 127.68, 122.73, 121.97, 120.69, 118.42, 115.37, 112.31, 108.46, 28.75, 26.11; IR ($CHCl_3$): ν_{max} 3390, 2953, 2918, 1653, 1558, 1492, 1457, 1428, 1401, 1243, 1226, 1102, 1021 cm^{-1} ; HR-ESIMS: m/z 255.1243 calcd for $C_{14}H_{14}N_4O + H^+$ (255.1240).

(E)-5-(Benzo[d][1,3]dioxol-5-ylmethylene)-2-imino-1,3-dimethylimidazolidin-4-one [(E)-**8a**]. Yield: 58%; pale yellow solid; m.p. 117–119 °C; HPLC purity: >99% ($t_R = 5.35$ min); 1H NMR ($CDCl_3$, 400 MHz): δ 7.71 (s, 1H), 7.19 (d, 1H, $J = 8.4$ Hz), 6.79 (d, 1H, $J = 8.4$ Hz), 5.98 (s, 3H), 3.21 (s, 3H), 3.15 (s, 3H); ^{13}C NMR ($CDCl_3$, 100 MHz): δ 161.72, 152.53, 147.65, 129.06, 127.41, 125.09, 113.31, 109.90, 107.94, 101.23, 27.06, 24.95; IR ($CHCl_3$): ν_{max} 3339, 2923, 1725, 1658, 1487, 1433, 1397, 1359, 1322, 1300, 1259, 1239, 1196, 1136, 1089, 1037 cm^{-1} ; HR-ESIMS: m/z 260.1035 calcd for $C_{13}H_{13}N_3O_3 + H^+$ (260.1030).

(Z)-5-(Benzo[d][1,3]dioxol-5-ylmethylene)-2-imino-1,3-dimethylimidazolidin-4-one [(Z)-**8a**]. Yield: 63%; pale yellow solid; m.p. 148–150 °C; HPLC purity: 96% ($t_R = 5.4$ min); 1H NMR ($CDCl_3$, 400 MHz): δ 6.81–6.77 (m, 3H), 6.60 (s, 1H), 5.99 (s, 2H), 3.18 (s, 3H), 3.04 (s, 3H); ^{13}C NMR ($CDCl_3$, 125 MHz): δ 163.84, 155.04, 147.58, 147.41, 130.13, 127.12, 123.58, 109.54, 108.27, 108.22, 101.35, 31.77, 25.51; IR ($CHCl_3$): ν_{max} 3316, 2922, 1734, 1674, 1646, 1501, 1487, 1441, 1395, 1351, 1316, 1260, 1241, 1136, 1120, 1098, 1036 cm^{-1} ; HR-ESIMS: m/z 260.1024 calcd for $C_{13}H_{13}N_3O_3 + H^+$ (260.1030).

(E)-2-Imino-1,3-dimethyl-5-(naphthalen-1-ylmethylene)imidazolidin-4-one [(E)-**8b**]. Yield: 45%; pale yellow solid; m.p. 103–105 °C; HPLC purity: 93% ($t_R = 11.9$ min); 1H NMR ($CDCl_3$, 400 MHz): δ 7.93–7.86 (m, 4H), 7.57–7.52 (m, 2H), 7.49 (d, 1H, $J = 8.0$ Hz), 7.36 (d, 1H, $J = 7.2$ Hz), 7.31 (s, 1H), 3.18 (s, 3H), 2.73 (s, 3H); ^{13}C NMR ($CDCl_3$, 125 MHz): δ 163.54, 155.67, 133.29, 132.05, 131.18, 129.99, 129.05, 128.63, 127.50, 126.85, 126.50, 125.29, 124.79, 110.17, 29.66, 25.12; IR ($CHCl_3$): ν_{max} 3428, 3056, 2924, 2852, 1766, 1720, 1663, 1589, 1507, 1467, 1432, 1392, 1309, 1262, 1221, 1159, 1126, 1102, 1083, 1053, 1037, 1017 cm^{-1} ; HR-ESIMS: m/z 266.1280 calcd for $C_{16}H_{15}N_3O + H^+$ (266.1288).

(E)-2-Imino-1,3-dimethyl-5-(naphthalen-2-ylmethylene)imidazolidin-4-one [(E)-**8c**]. Yield: 32%; off-white solid; m.p. 309–311 °C; HPLC purity: 93% ($t_R = 5.32$ min); 1H NMR ($DMSO-d_6$, 400 MHz): δ 8.53 (s, 1H), 8.39 (d, 1H, $J = 8.8$ Hz), 8.05 (d, 1H, $J = 4.0$ Hz), 7.87–7.83 (m, 3H), 7.51–7.48 (m, 2H), 6.42 (s, 1H), 3.22 (s, 3H), 2.95 (s, 3H); ^{13}C NMR

(CDCl₃ + CD₃OD, 125 MHz): δ 134.61, 134.57, 132.25, 131.33, 129.69, 129.26, 128.74, 128.60, 127.77, 127.34, 118.68, 117.22, 30.27, 28.67; IR (CHCl₃): ν_{\max} 3400, 2922, 2853, 1662, 1588, 1568, 1454, 1408, 1383, 1345, 1297, 1270, 1243, 1206, 1145, 1049, 1021 cm⁻¹; HR-ESIMS: m/z 266.1286 calcd for C₁₆H₁₅N₃O + H⁺ (266.1288).

(*E*)-5-(Anthracen-9-ylmethylene)-2-imino-1,3-dimethylimidazolidin-4-one [(*E*)-8d]. Yield: 47%; pale yellow solid; m.p. 247–249 °C; HPLC purity: >99% (t_R = 6.13 min); ¹H NMR (CDCl₃, 500 MHz): δ 8.45 (s, 1H), 8.02–7.99 (m, 4H), 7.46–7.44 (m, 4H), 6.82 (s, 1H), 3.42 (s, 3H), 2.93 (s, 3H); ¹³C NMR (CDCl₃, 125 MHz): δ 160.82, 154.29, 132.63, 131.27, 129.95, 129.04, 127.75, 126.63, 125.97, 125.24, 125.22, 109.73, 26.66, 24.61; IR (CHCl₃): ν_{\max} 3415, 2924, 2853, 1769, 1722, 1658, 1449, 1391, 1273, 1128, 1106, 1073, 1043 cm⁻¹; HR-ESIMS: m/z 316.1438 calcd for C₂₀H₁₇N₃O + H⁺ (316.1444).

(*Z*)-5-(Anthracen-9-ylmethylene)-2-imino-1,3-dimethylimidazolidin-4-one [(*Z*)-8d]. Yield: 38%; pale yellow solid; m.p. 142–144 °C; HPLC purity: >99% (t_R = 6.27 min); ¹H NMR (CDCl₃, 400 MHz): δ 8.50 (s, 1H), 8.06–8.0 (m, 4H), 7.52 (s, 5H), 3.23 (s, 3H), 2.27 (s, 3H); ¹³C NMR (CDCl₃, 125 MHz): δ 163.12, 155.42, 132.63, 130.97, 130.33, 128.94, 127.99, 126.58, 126.18, 125.67, 125.62, 108.36, 28.06, 25.17; IR (CHCl₃): ν_{\max} 3433, 3052, 2925, 2854, 1770, 1724, 1667, 1623, 1519, 1443, 1392, 1297, 1271, 1222, 1128, 1106, 1073, 1044, 1016 cm⁻¹; HR-ESIMS: m/z 316.1438 calcd for C₂₀H₁₇N₃O + H⁺ (316.1444).

(*E*)-5-(2,3-Dimethoxybenzylidene)-2-imino-1,3-dimethylimidazolidin-4-one [(*E*)-8e]. Yield: 59%; off-white solid; m.p. 107–109 °C; HPLC purity: 99% (t_R = 6.96 min); ¹H NMR (CDCl₃, 400 MHz): δ 7.73 (dd, 1H, J = 8.0, 1.2 Hz), 7.07 (t, 1H, J = 8.0 Hz), 6.93 (dd, 1H, J = 8.8, 1.2 Hz), 6.57 (s, 1H), 3.88 (s, 3H), 3.84 (s, 3H), 3.25 (s, 3H), 3.10 (s, 3H); ¹³C NMR (CDCl₃, 125 MHz): δ 161.67, 153.79, 152.32, 147.66, 129.71, 126.65, 123.44, 122.73, 113.37, 111.39, 61.17, 55.85, 26.48, 24.64; IR (CHCl₃): ν_{\max} 3416, 2923, 2852, 1762, 1714, 1633, 1576, 1475, 1454, 1425, 1392, 1293, 1266, 1224, 1169, 1102, 1080, 1050, 1009 cm⁻¹; HR-ESIMS: m/z 276.1350 calcd for C₁₄H₁₇N₃O₃ + H⁺ (276.1343).

(*Z*)-5-(2,3-Dimethoxybenzylidene)-2-imino-1,3-dimethylimidazolidin-4-one [(*Z*)-8e]. Yield: 43%; off-white solid; m.p. 103–105 °C; HPLC purity: 98% (t_R = 7.16 min); ¹H NMR (CDCl₃, 400 MHz): δ 7.06 (t, 1H, J = 8.0 Hz), 6.92 (d, 2H, J = 9.6 Hz), 6.78 (d, 1H, J = 7.2 Hz), 3.89 (s, 3H), 3.81 (s, 3H), 3.14 (s, 3H), 2.94 (s, 3H); ¹³C NMR (CDCl₃, 125 MHz): δ 163.63, 155.80, 152.71, 147.55, 130.54, 127.18, 123.57, 122.55, 112.75, 108.16, 60.73, 55.82, 29.69, 25.02; IR (CHCl₃): ν_{\max} 3416, 2921, 2851, 1769, 1721, 1665, 1577, 1471, 1432, 1393, 1318, 1275, 1127, 1076, 1050 cm⁻¹; HR-ESIMS: m/z 276.1357 calcd for C₁₄H₁₇N₃O₃ + H⁺ (276.1343).

(*E*)-2-Imino-1,3-dimethyl-5-(2,4,5-trimethoxybenzylidene)imidazolidin-4-one [(*E*)-8f]. Yield: 67%; pale yellow solid; m.p. 178–180 °C; HPLC purity: 97% (t_R = 6.26 min); ¹H NMR (CDCl₃, 400 MHz): δ 8.38 (s, 1H), 6.69 (s, 1H), 6.49 (s, 1H), 3.94 (s, 6H), 3.88 (s, 3H), 3.25 (s, 3H), 3.13 (s, 3H); ¹³C NMR (CDCl₃, 125 MHz): δ 162.17, 153.62, 152.98, 151.10, 142.42, 126.88, 113.60, 113.19, 112.25, 96.04, 56.51, 56.40, 56.01, 26.47, 24.69; IR (CHCl₃): ν_{\max} 3400, 2955, 2922, 2852, 1760, 1715, 1658, 1608, 1512, 1464, 1394, 1344, 1318, 1284, 1209, 1113, 1097, 1029 cm⁻¹; GC-MS (EI) m/z (%): 307.3 (5.57), 306.3 (M⁺+1, 35.73), 284.2 (2.99), 281.2 (7.47), 275.3 (1.18), 260.2 (2.99), 231.2 (4.75), 209.1 (4.75), 206.2 (18.2), 178.2 (9.78), 137.2 (5.43), 110.97 (5.42), 97.1 (5.43).

(*Z*)-2-Imino-1,3-dimethyl-5-(2,4,5-trimethoxybenzylidene)imidazolidin-4-one [(*Z*)-8f]. Yield: 51%; pale yellow solid; m.p. 157–159 °C; HPLC purity: 98% (t_R = 6.03 min); ¹H NMR (CDCl₃, 400 MHz): δ 6.90 (s, 1H), 6.71 (s, 1H), 6.52 (s, 1H), 3.93 (s, 3H), 3.84 (s, 6H), 3.13 (s, 3H), 3.02 (s, 3H); ¹³C NMR (CDCl₃, 100 MHz): δ 163.79, 156.13, 152.72, 150.67, 142.57, 129.36, 114.30, 112.73, 108.88, 96.94, 56.65, 56.23, 56.12, 30.03, 24.95; IR (CHCl₃): ν_{\max} 3426, 2954, 2925, 2852, 1761, 1716, 1659, 1608, 1582, 1511, 1465, 1343, 1313, 1284, 1208, 1113, 1029 cm⁻¹; GC-MS (EI) m/z (%): 306.3 (M⁺+1, 94.01), 291.3 (17.35), 275.3 (37.58), 260.3 (10.92), 231.2 (9.1), 206.2 (60.67), 178.2 (27), 174.2 (14.09), 162.2 (6.05), 137.3 (9.1), 110.7 (8.45), 92.1 (7.45), 63.1

(7.05).

(*E*)-5-(4-Chlorobenzylidene)-2-imino-1,3-dimethylimidazolidin-4-one [(*E*)-8g]. Yield: 87%; off-white solid; m.p. 122–124 °C; HPLC purity: 98% (t_R = 10.77 min); ¹H NMR (CDCl₃, 500 MHz): δ 7.85 (d, 2H, J = 8.5 Hz), 7.34 (d, 2H, J = 8.5 Hz), 6.15 (s, 1H), 3.22 (s, 3H), 3.11 (s, 3H); ¹³C NMR (CDCl₃, 125 MHz): δ 161.67, 153.63, 134.76, 131.54, 130.93, 129.59, 128.46, 115.56, 26.41, 24.73; IR (CHCl₃): ν_{\max} 3391, 2954, 2919, 2848, 1752, 1707, 1632, 1491, 1452, 1426, 1387, 1347, 1296, 1269, 1089, 1050, 1014 cm⁻¹; GC-MS (EI) m/z (%): 252.1 (35.62), 250.2 (M⁺, 96.24), 249.3 (19.86), 165.2 (81.18), 152.2 (32.9), 151.2 (8.96), 150.2 (99.7), 123.2 (22.79), 114.2 (10.14), 89 (10.71), 63 (9.21).

(*Z*)-5-(4-Chlorobenzylidene)-2-imino-1,3-dimethylimidazolidin-4-one [(*Z*)-8g]. Yield: 63%; off-white solid; m.p. 95–97 °C; HPLC purity: 98% (t_R = 10.36 min); ¹H NMR (CDCl₃, 400 MHz): δ 7.37 (d, 2H, J = 8.4 Hz), 7.23 (d, 2H, J = 8.4 Hz), 6.86 (s, 1H), 3.14 (s, 3H), 2.96 (s, 3H); ¹³C NMR (CDCl₃, 125 MHz): δ 163.58, 155.83, 134.44, 131.14, 130.73, 130.16, 128.54, 110.68, 30.46, 25.12; IR (CHCl₃): ν_{\max} 3429, 2924, 2853, 1830, 1770, 1721, 1662, 1592, 1489, 1464, 1435, 1393, 1315, 1269, 1212, 1123, 1094, 1052, 1014 cm⁻¹; GC-MS (EI) m/z (%): 252.1 (30.48), 251.2 (M⁺+1, 20.02), 250.2 (M⁺, 99.96), 166.2 (8.19), 165.2 (76.95), 152.3 (29.79), 150.3 (94.75), 123.3 (21.94), 114.3 (9.83), 103.2 (8.49), 89 (10.67), 63 (7.45).

(*E*)-5-(3-Bromobenzylidene)-2-imino-1,3-dimethylimidazolidin-4-one [(*E*)-8h]. Yield: 75%; brown solid; m.p. 156–158 °C; HPLC purity: 98% (t_R = 11.33 min); ¹H NMR (CDCl₃, 400 MHz): δ 8.08 (s, 1H), 7.81 (d, 1H, J = 8.0 Hz), 7.46 (d, 1H, J = 8.0 Hz), 7.24 (d, 1H, J = 8.0 Hz), 6.13 (s, 1H), 3.23 (s, 3H), 3.12 (s, 3H); ¹³C NMR (CDCl₃, 100 MHz): δ 161.52, 153.61, 134.48, 132.82, 131.67, 130.19, 129.66, 128.73, 122.19, 114.86, 26.40, 24.74; IR (CHCl₃): ν_{\max} 3411, 3048, 2920, 1758, 1709, 1628, 1588, 1556, 1462, 1428, 1394, 1340, 1297, 1273, 1102, 1077, 1054 cm⁻¹; GC-MS (EI) m/z (%): 296.1 (M⁺+1, 99.93), 295.3 (33.94), 293.7 (16.69), 215.2 (13.9), 209.2 (64.78), 194.3 (47.4), 167.2 (6.35), 115.2 (30.53), 114.3 (17.91), 102.2 (8.49), 89.0 (20), 63.0 (12.07).

(*Z*)-5-(3-Bromobenzylidene)-2-imino-1,3-dimethylimidazolidin-4-one [(*Z*)-8h]. Yield: 67%; pale yellow solid; m.p. 113–115 °C; HPLC purity: 98% (t_R = 11.21 min); ¹H NMR (CDCl₃, 400 MHz): δ 7.49–7.45 (m, 2H), 7.25–7.21 (m, 2H), 6.84 (s, 1H), 3.14 (s, 3H), 2.96 (s, 3H); ¹³C NMR (CDCl₃, 125 MHz): δ 163.44, 155.71, 134.76, 132.18, 131.31, 130.46, 129.68, 127.95, 122.27, 110.06, 30.43, 25.10; IR (CHCl₃): ν_{\max} 3427, 2953, 2922, 2851, 1769, 1720, 1659, 1592, 1558, 1467, 1433, 1392, 1311, 1268, 1120, 1092, 1071, 1052 cm⁻¹; GC-MS (EI) m/z (%): 296.1 (M⁺+1, 99.97), 295.3 (33.26), 293.6 (19.48), 215.1 (14.06), 209.2 (66.36), 194.3 (51.65), 169.2 (6.65), 115.2 (31.6), 114.2 (18.95), 103.2 (8.34), 89.0 (18.78), 63.0 (14.15).

(*E*)-5-(2,4-Dichlorobenzylidene)-2-imino-1,3-dimethylimidazolidin-4-one [(*E*)-8i]. Yield: 82%; off-white solid; m.p. 168–170 °C; HPLC purity: 97% (t_R = 14.64 min); ¹H NMR (CDCl₃, 500 MHz): δ 7.94 (d, 1H, J = 8.5 Hz), 7.42 (d, 1H, J = 2.0 Hz), 7.25 (dd, 1H, J = 8.5, 2.0 Hz), 6.35 (s, 1H), 3.25 (s, 3H), 3.09 (s, 3H); ¹³C NMR (CDCl₃, 125 MHz): δ 161.51, 153.65, 135.03, 134.69, 132.33, 130.68, 129.16, 129.02, 126.67, 110.88, 26.47, 24.73; IR (CHCl₃): ν_{\max} 3410, 3073, 2920, 1766, 1717, 1650, 1584, 1548, 1471, 1449, 1426, 1391, 1334, 1303, 1266, 1093, 1046 cm⁻¹; GC-MS (EI) m/z (%): 252.1 (3.92), 251.1 (31.37), 250.2 (11.71), 249.4 (100), 234.6 (4.43), 184.4 (14.81), 157.3 (6.9), 114.3 (4.42).

4.4. General procedure for synthesis of indolic NH-substituted aplysinopsin analogs 5a-5c

The solution of aplysinopsin (**1**, 1 equiv.) in methylene chloride was stirred at room temperature. DMAP (0.05 equiv.), aryl sulfonyl chloride (1.1 equiv.) and *N,N*-diisopropylethylamine (1.5 equiv.) were added to this solution, and reaction was allowed to stir at rt for 20 h. After completion of the reaction, 10% HCl was added, and product was extracted with methylene chloride. The solvent was evaporated on rotavapor, and the obtained crude product was purified by silica gel

chromatography to get the titled products **5a-5c**.

(*E*)-2-Imino-1,3-dimethyl-5-((1-tosyl-1*H*-indol-3-yl)methylene)imidazolidin-4-one (**5a**). Yield: 42%; pale brown solid; m.p. 244–266 °C; HPLC purity: 99% ($t_R = 10.25$ min); ^1H NMR (CDCl_3 , 400 MHz): δ 9.02 (s, 1H), 8.03 (d, 1H, $J = 8.0$ Hz), 7.86 (d, 2H, $J = 8.4$ Hz), 7.59 (d, 1H, $J = 7.6$ Hz), 7.36–7.29 (m, 3H), 7.22 (d, 2H, $J = 8.4$ Hz), 6.07 (s, 1H), 3.28 (s, 3H), 3.22 (s, 3H), 2.32 (s, 3H); ^{13}C NMR (CDCl_3 , 125 MHz): δ 161.96, 152.44, 144.93, 135.26, 135.18, 134.43, 130.65, 130.23, 129.91, 129.89, 127.51, 127.01, 124.82, 123.31, 118.26, 114.35, 113.84, 99.96, 27.06, 25.07, 21.57; IR (CHCl_3): ν_{max} 3340, 2923, 2853, 1726, 1667, 1633, 1448, 1433, 1399, 1373, 1306, 1262, 1173, 1213, 1188, 1097, 1020 cm^{-1} ; HR-ESIMS: m/z 409.1324 calcd for $\text{C}_{21}\text{H}_{20}\text{N}_4\text{O}_3\text{S} + \text{H}^+$ (409.1329).

(*E*)-2-Imino-5-((1-((4-methoxyphenyl)sulfonyl)-1*H*-indol-3-yl)methylene)-1,3-dimethylimidazolidin-4-one (**5b**). Yield: 45%; pale yellow solid; m.p. 259–261 °C; HPLC purity: 99% ($t_R = 12.03$ min); ^1H NMR ($\text{DMSO}-d_6$, 400 MHz): δ 8.90 (s, 1H), 7.89 (t, 2H, $J = 7.2$ Hz), 7.82 (d, 2H, $J = 8.8$ Hz), 7.35–7.25 (m, 3H), 7.03 (d, 2H, $J = 8.8$ Hz), 6.16 (s, 1H), 3.71 (s, 3H), 3.19 (s, 3H), 3.04 (s, 3H); ^{13}C NMR (CDCl_3 , 125 MHz): δ 163.75, 161.65, 152.47, 134.09, 130.60, 129.24, 127.51, 124.77, 123.24, 118.23, 114.45, 113.78, 100.11, 55.60, 27.05, 25.06; IR (CHCl_3): ν_{max} 3445, 2080, 1634, 1165, 1018 cm^{-1} ; HR-ESIMS: m/z 425.1275 calcd for $\text{C}_{21}\text{H}_{20}\text{N}_4\text{O}_4\text{S} + \text{H}^+$ (425.1278).

(*E*)-2-Imino-1,3-dimethyl-5-((1-(naphthalen-2-ylsulfonyl)-1*H*-indol-3-yl)methylene)imidazolidin-4-one (**5c**). Yield: 34%; pale yellow solid; m.p. 224–226 °C; HPLC purity: >99% ($t_R = 9.78$ min); ^1H NMR ($\text{CDCl}_3 + \text{CD}_3\text{OD}$, 400 MHz): δ 9.11 (s, 1H), 8.63 (s, 1H), 8.10 (d, $J = 8.8$ Hz, 1H), 8.01 (d, $J = 7.2$ Hz, 1H), 7.89–7.84 (m, 3H), 7.65–7.61 (m, 3H), 7.38–7.31 (m, 3H), 6.25 (s, 1H), 3.32 (s, 3H), 3.26 (s, 3H); ^{13}C NMR ($\text{CDCl}_3 + \text{CD}_3\text{OD}$, 125 MHz): δ 135.22, 134.53, 134.30, 131.80, 130.48, 129.72, 129.67, 129.43, 129.42, 128.68, 127.78, 127.71, 127.67, 125.0, 123.53, 121.35, 118.37, 114.39, 113.60, 27.0, 24.95; IR (CHCl_3): ν_{max} 3391, 2955, 2923, 2853, 1650, 1463, 1384, 1020 cm^{-1} ; HR-ESIMS: m/z 445.1331 calcd for $\text{C}_{24}\text{H}_{20}\text{N}_4\text{O}_3\text{S} + \text{H}^+$ (445.1329).

4.5. *In vitro* AChE and BChE inhibition assay

The anti-cholinesterase effect of test compounds was determined using Ellman assay as described in our earlier publications [16,34,35]. The AChE from electric eel and BChE from equine serum were used for all inhibition studies. The enzyme inhibition constants and the type of inhibition (kinetics studies) for inhibition of rHuAChE and eqBChE was also performed as described earlier [16,34,35].

4.6. Fluorescence resonance energy transfer (FRET) assay

The inhibition of BACE-1 enzyme by test compounds was determined by a fluorescent based FRET assay, as described earlier [16]. The kinetic study of (Z)-**8g** with BACE-1 was performed using five different concentrations of the substrate (0.625–1 μM for each concentration of (Z)-**8g**). Five concentrations of (Z)-**8g** (0.3125–10 μM) and a parallel control with no inhibitor in the mixture were used for the study. To a 96 well black polystyrene microplate 10 μL test compound, 20 μL substrate and 68 μL FAB were added. The fluorimeter was set on well plate reader mode with respective excitation and emission wavelengths at 320 nm and 405 nm. Initial fluorescence was measured immediately after the addition of two microliter BACE-1 enzyme. The plate was then covered and incubated for 4 hr at 37 °C. After 4 hr of incubation, final fluorescence was measured. Difference between the initial and final fluorescence readings gives Δ fluorescence which is used for calculations. Background signal pertaining to the substrate was measured in control wells and was subtracted.

4.7. Propidium iodide displacement assay

Binding of the test compounds to the PAS of AChE can be determined

by propidium-iodide displacement assay via competitive displacement of propidium iodide by the compounds. Tris HCl (1 mM, pH 8.0) is used as the buffer for dilutions in the assay. Briefly 5U of EeAChE was incubated with/without test compounds (150 μL , final concentrations of 10 and 50 μM) at 25 °C for 6 h. Propidium iodide (1 μM , 50 μL) was added and the assay mixture was incubated for 10 min at 25 °C. The fluorometer was set on well plate reader mode with excitation at 535 nm and emission at 595 nm, respectively. After incubation, fluorescence intensities were measured. The background signal was measured from control wells containing all reagents (except EeAChE) and was subtracted. Each concentration was assayed in triplicate. The percentage inhibition was calculated using the following formula: $100 - (\text{IF}_i/\text{IF}_0 \times 100)$, where IF_i and IF_0 are the fluorescence intensities with and without inhibitor, respectively.

4.8. *In vitro* BBB permeation assay

Test compound was dissolved in DMSO at 5 mg/mL concentration, and was further diluted with PBS buffer (pH 7.4) to 50 $\mu\text{g}/\text{mL}$. The filter membrane of donor plate was coated with PBL in dodecane (selected empirically as 4 μL volume of 20 mg/mL PBL in dodecane). To this plate was added, 0.2 ml of test compound solution. The acceptor plate was also filled with 0.15 ml of PBS buffer (pH 7.4), and it was carefully put below the donor plate to form a 'sandwich'. The plate was kept at 25 °C, for 18 hrs. The concentration of test sample in the donor and acceptor wells was determined using UV plate reader, at the respective λ_{max} of the test compound. The assay was first validated using three known drugs, which were covering the permeability (P_e , $\times 10^{-6}$ cm/s) range of 1–12. Donepezil was used as a high permeability standard and theophylline as a low permeability standard. The effective permeability coefficient (P_e) of the compound was calculated by using following equation [42].

$$P_e = Cx - \text{Ln} \left(1 - \frac{[\text{drug}]_{\text{acceptor}}}{[\text{drug}]_{\text{equilibrium}}} \right)$$

where $C = (V_D \times V_A)/(V_D + V_A) \times \text{Area} \times \text{Time}$. Here, V_D and V_A are the volume of solution in the donor side and acceptor side, respectively. Area is the membrane area, and Time is the incubation time of the experiment.

4.9. A β 42 self-aggregation inhibition assay

Amyloid beta 1–42 rat peptide (Sigma-Aldrich, Saint Louis) was dissolved in 10% (w/v) ammonium hydroxide (NH_4OH) at a concentration of 0.5 mg/ml. This peptide solution was incubated for ten minutes at room temperature followed by removal of NH_4OH using vacuum concentrator resulting in a fluffy white peptide [43]. Immediately before the assay, NH_4OH pretreated A β 42 was reconstituted in a mixture of $\text{CH}_3\text{CN}/0.3$ mM $\text{Na}_2\text{CO}_3/250$ mM NaOH (48.4:48.4:3.2) to obtain a 200 μM solution. Aggregation assays were performed by incubating the peptide with and without inhibitors (final A β and inhibitor concentrations of 20 and 10 μM , respectively) in phosphate buffer (10 mM, pH = 8.0) containing 10 mM NaCl, for 24 h at 30 °C (A β /inhibitor = 2/1). All the assays were carried out in duplicate in 96-well black microtiter plates. Thioflavin T (ThT) fluorescence method was used for the quantification of amyloid fibrils formation. After the incubation period ThT was added to the assay solutions at a final concentration of 40 μM (final assay volume: 200 μL) and fluorescence intensity was recorded with 446/490 nm excitation/emission filters set for 300 s at an interval of 30 s [44]. Blanks containing only tested inhibitors and ThT were also checked simultaneously for subtracting the background signal. The percentage inhibition due to the presence of test compound was calculated by the following expression: $100 - (\text{IF}_i/\text{IF}_0 \times 100)$ where IF_i and IF_0 are the respective fluorescence intensities obtained in the presence and in the absence of inhibitor, respectively.

4.10. Molecular modelling

The crystal structure of human AChE (PDB ID: 4EY7) [45], human BChE (PDB ID: 6EP4) [46] and BACE-1 (PDB: 4B05) [8] were retrieved from protein data bank and were used for molecular modelling studies under default settings from Glide. The docking was performed as described earlier [16].

Declaration of Competing Interest

The authors declare that they have no known competing financial interests or personal relationships that could have appeared to influence the work reported in this paper.

Acknowledgement

R.R.Y. thanks CSIR for Senior Research Fellowship. Authors are thankful to the analytical department, IIIM, for analytical support. The authors acknowledge the financial support from the Department of Biotechnology (DBT) grant number BT/PR15735/AAQ/3/793/2016 (GAP-2159).

Author contributions

R.R. Yadav synthesized all compounds. V.K. Nuthakki performed all biological experiments; S.B. Bharate performed molecular modeling. S. B. Bharate designed and monitored whole study. All three authors contributed to manuscript writing.

IIIM Publication number: CSIR-IIIM/IPR/00131.

Declaration of Competing Interest

The authors declare that they have no known competing financial interests or personal relationships that could have appeared to influence the work reported in this paper.

Appendix A. Supplementary material

NMR spectra scans for all compounds. Supplementary data to this article can be found online at <https://doi.org/10.1016/j.bioorg.2020.104568>.

References

- [1] Dementia fact sheet, 2017. <https://www.who.int/news-room/fact-sheets/detail/dementia> (accessed on December 15, 2020), World Health Organization.
- [2] C.A. Lane, J. Hardy, J.M. Schott, *Alzheimer's disease*, *Eur. J. Neurol.* 25 (1) (2018) 59–70.
- [3] P. Scheltens, K. Blennow, M.M.B. Breteler, B. de Strooper, G.B. Frisoni, S. Salloway, W.M. Van der Flier, *Alzheimer's disease*, *The Lancet* 388 (10043) (2016) 505–517.
- [4] J. Hardy, D.J. Selkoe, The amyloid hypothesis of Alzheimer's disease: progress and problems on the road to therapeutics, *Science* 297 (5580) (2002) 353–356.
- [5] M.A. Maia, E. Sousa, BACE-1 and gamma-secretase as therapeutic targets for Alzheimer's disease, *Pharmaceuticals (Basel)* 12 (1) (2019), <https://doi.org/10.3390/ph12010041>.
- [6] S.L. Roberds, J. Anderson, G. Basi, M.J. Bienkowski, D.G. Branstetter, K.S. Chen, S. B. Freedman, N.L. Frigon, D. Games, K. Hu, K. Johnson-Wood, K.E. Kappelman, T. T. Kawabe, I. Kola, R. Kuehn, M. Lee, W. Liu, R. Motter, N.F. Nichols, M. Power, D. W. Robertson, D. Schenk, M. Schoor, G.M. Shopp, M.E. Shuck, S. Sinha, K. A. Svensson, G. Tatsuno, H. Tintrup, J. Wijsman, S. Wright, L. McConlogue, BACE knockout mice are healthy despite lacking the primary beta-secretase activity in brain: implications for Alzheimer's disease therapeutics, *Hum. Mol. Genet.* 10 (12) (2001) 1317–1324.
- [7] D. Kumar, A. Ganeshpurkar, D. Kumar, G. Modi, S.K. Gupta, S.K. Singh, Secretase inhibitors for the treatment of Alzheimer's disease: long road ahead, *Eur. J. Med. Chem.* 148 (2018) 436–452.
- [8] F. Jeppsson, S. Eketjäll, J. Janson, S. Karlstrom, S. Gustavsson, L.L. Olsson, A. C. Radesater, B. Ploeger, G. Cebers, K. Kolmodin, B.M. Swahn, S. von Berg, T. Bueters, J. Falting, Discovery of AZD3839, a potent and selective BACE1 inhibitor clinical candidate for the treatment of Alzheimer disease, *J. Biol. Chem.* 287 (49) (2012) 41245–41257.
- [9] Y. Chen, J. Sun, L. Fang, M. Liu, S. Peng, H. Liao, J. Lehmann, Y. Zhang, Tacrine–ferulic acid–nitric oxide (NO) donor trihybrids as potent, multifunctional acetyl- and butyrylcholinesterase inhibitors, *J. Med. Chem.* 55 (9) (2012) 4309–4321.
- [10] Q. Li, H. Yang, Y. Chen, H. Sun, Recent progress in the identification of selective butyrylcholinesterase inhibitors for Alzheimer's disease, *Eur. J. Med. Chem.* 132 (2017) 294–309.
- [11] E. Giacobini, Cholinesterases: new roles in brain function and in Alzheimer's disease, *Neurochem. Res.* 28 (3–4) (2003) 515–522.
- [12] S. Darvesh, Butyrylcholinesterase as a diagnostic and therapeutic target for Alzheimer's disease, *Curr. Alzheimer Res.* 13 (10) (2016) 1173–1177.
- [13] R.M. Lane, S.G. Potkin, A. Enz, Targeting acetylcholinesterase and butyrylcholinesterase in dementia, *Int. J. Neuropsychopharmacol.* 9 (1) (2006) 101–124.
- [14] N.H. Greig, D.K. Lahiri, K. Sambamurti, Butyrylcholinesterase: an important new target in Alzheimer's disease therapy, *Int. Psychogeriatr.* 14 (Suppl 1) (2002) 77–91.
- [15] P. Zhang, S. Xu, Z. Zhu, J. Xu, Multi-target design strategies for the improved treatment of Alzheimer's disease, *Eur. J. Med. Chem.* 176 (2019) 228–247.
- [16] V.K. Nuthakki, A. Sharma, A. Kumar, S.B. Bharate, Identification of embelin, a 3-undecyl-1,4-benzoquinone from *Embelia ribes* as a multitargeted anti-Alzheimer agent, *Drug Dev. Res.* 80 (5) (2019) 655–665.
- [17] S.B. Bharate, S.D. Sawant, P.P. Singh, R.A. Vishwakarma, Kinase inhibitors of marine origin, *Chem. Rev.* 113 (8) (2013) 6761–6815.
- [18] R. Kazlauskas, P.T. Murphy, R.J. Quinn, R.J. Wells, Aplysinopsin, a new tryptophan derivative from a sponge, *Tetrahedron Lett.* 18 (1) (1977) 61–64.
- [19] K.H. Hollenbeak, F.J. Schmitz, Aplysinopsin: antineoplastic tryptophan derivative from the marine sponge *Verongia spengelii*, *Lloydia* 40 (5) (1977) 479–481.
- [20] P. Djura, D.J. Faulkner, Metabolites of the marine sponge *Dercitus species*, *J. Org. Chem.* 45 (4) (1980) 735–737.
- [21] J.-F. Hu, J.A. Schetz, M. Kelly, J.-N. Peng, K.K.H. Ang, H. Flotow, C.Y. Leong, S. B. Ng, A.D. Buss, S.P. Wilkins, M.T. Hamann, New anti-infective and human 5-HT2 receptor binding natural and semisynthetic compounds from the Jamaican Sponge *Smenospongia aurea*, *J. Nat. Prod.* 65 (4) (2002) 476–480.
- [22] A.A. Tymiak, K.L. Rinehart Jr, G.J. Bakus, Constituents of morphologically similar sponges: *Aplysina* and *smenospongia* species, *Tetrahedron* 41 (6) (1985) 1039–1047.
- [23] E. Fattorusso, V. Lanzotti, S. Magno, E. Novellino, Tryptophan derivatives from a Mediterranean anthozoan, *Astroides calycularis*, *J. Nat. Prod.* 48 (6) (1985) 924–927.
- [24] R.K. Okuda, D. Klein, R.B. Kinnel, M. Li, P. Scheuer, Marine natural products: the past twenty years and beyond, *Pure Appl. Chem.* 54 (1982) 1907–1914.
- [25] N.L. Segraves, P. Crews, Investigation of brominated tryptophan alkaloids from two thorectandra and Smenospongia, *J. Nat. Prod.* 68 (10) (2005) 1484–1488.
- [26] G. Guella, I. Mancini, H. Zibrowius, F. Pietra, Aplysinopsin-type alkaloids from *Dendrophyllia* sp., a scleractinian coral of the family dendrophylliidae of the Philippines, facile photochemical (Z/E) photoisomerization and thermal reversal, *Helv. Chim. Acta* 72 (7) (1989) 1444–1450.
- [27] G. Guella, I. Mancini, H. Zibrowius, F. Pietra, Novel aplysinopsin-type alkaloids from scleractinian corals of the family dendrophylliidae of the mediterranean and the Philippines. Configurational-assignment criteria, stereospecific synthesis, and photoisomerization, *Helv. Chim. Acta* 71 (4) (1988) 773–782.
- [28] R.J. Wells, New metabolites from Australian marine species, *Pure Appl. Chem.* 51 (1979) 1829–1846.
- [29] K. Kondo, J. Nishi, M. Ishibashi, J. Kobayashi, Two new tryptophan-derived alkaloids from the Okinawan marine sponge *Aplysina* sp. *J. Nat. Prod.* 57 (7) (1994) 1008–1011.
- [30] S.N. Singh, S. Bhatnagar, N. Fatma, P.M.S. Chauhan, R.K. Chatterjee, Antifilarial activity of a synthetic marine alkaloid, aplysinopsin (CDRI Compound 92/138), *Trop. Med. Int. Health* 2 (6) (1997) 535–543.
- [31] D. Gulati, P.M.S. Chauhan, R.P. Bhakuni, D.S. Bhakuni, A new synthesis of aplysinopsin, a marine alkaloid and its analogues and their biological activities, *Indian J. Chem.* 33B (1993) 4–9.
- [32] J. Baird-Lambert, P.A. Davis, K.M. Taylor, Methylaplysinopsin: a natural product of marine origin with effects on serotonergic neurotransmission, *Clin. Exp. Pharmacol. Physiol.* 9 (2) (1982) 203–212.
- [33] G.L. Kenyon, G.L. Rowley, Tautomeric preferences among glycoamidines, *J. Am. Chem. Soc.* 93 (21) (1971) 5552–5560.
- [34] N. Augustin, V.K. Nuthakki, M. Abdullaha, Q.P. Hassan, S.G. Gandhi, S.B. Bharate, Discovery of helminthosporin, an anthraquinone isolated from *Rumex abyssinicus* Jacq as a dual cholinesterase inhibitor, *ACS Omega* 5 (3) (2020) 1616–1624.
- [35] V.K. Nuthakki, R. Mudududdla, A. Sharma, A. Kumar, S.B. Bharate, Synthesis and biological evaluation of indoloquinoline alkaloid cryptolepine and its bromo-derivative as dual cholinesterase inhibitors, *Bioorg. Chem.* 90 (2019) 103062.
- [36] M.F. Egan, J. Kost, P.N. Tariot, P.S. Aisen, J.L. Cummings, B. Vellas, C. Sur, Y. Mukai, T. Voss, C. Furtek, E. Mahoney, L. Harper Mozley, R. Vandenberghe, Y. Mo, D. Michelson, Randomized trial of verubecestat for mild-to-moderate Alzheimer's disease, *N. Engl. J. Med.* 378 (18) (2018) 1691–1703.
- [37] G.L. Ellman, K.D. Courtney, V. Andres, R.M. Featherstone, A new and rapid colorimetric determination of acetylcholinesterase activity, *Biochem. Pharmacol.* 7 (2) (1961) 88–95.
- [38] N. Nunes-Tavares, A. Nery da Matta, C.M. Batista e Silva, G.M. Araujo, S.R. Louro, A. Hason-Voloch, Inhibition of acetylcholinesterase from *Electrophorus electricus* (L.) by tricyclic antidepressants, *Int. J. Biochem. Cell Biol.* 34 (9) (2002) 1071–1079.

- [39] H. LeVine 3rd, Quantification of beta-sheet amyloid fibril structures with thioflavin T, *Methods Enzymol.* 309 (1999) 274–284.
- [40] K. Lewellyn, D. Bialonska, N.D. Chaurasiya, B.L. Tekwani, J.K. Zjawiony, Synthesis and evaluation of aplysinopsin analogs as inhibitors of human monoamine oxidase A and B, *Bioorg. Med. Chem. Lett.* 22 (15) (2012) 4926–4929.
- [41] K. Lewellyn, D. Bialonska, M.J. Loria, S.W. White, K.J. Sufka, J.K. Zjawiony, In vitro structure-activity relationships of aplysinopsin analogs and their in vivo evaluation in the chick anxiety-depression model, *Bioorg. Med. Chem.* 21 (22) (2013) 7083–7090.
- [42] L. Di, E.H. Kerns, K. Fan, O.J. McConnell, G.T. Carter, High throughput artificial membrane permeability assay for blood-brain barrier, *Eur. J. Med. Chem.* 38 (3) (2003) 223–232.
- [43] T.M. Ryan, J. Caine, H.D. Mertens, N. Kirby, J. Nigro, K. Breheny, L. J. Waddington, V.A. Streltsov, C. Curtain, C.L. Masters, B.R. Roberts, Ammonium hydroxide treatment of A β produces an aggregate free solution suitable for biophysical and cell culture characterization, *PeerJ* 1 (2013) e73.
- [44] M. Bartolini, C. Bertucci, M.L. Bolognesi, A. Cavalli, C. Melchiorre, V. Andrisano, Insight into the kinetic of amyloid beta (1–42) peptide self-aggregation: elucidation of inhibitors' mechanism of action, *ChemBioChem* 8 (17) (2007) 2152–2161.
- [45] J. Cheung, M.J. Rudolph, F. Burshteyn, M.S. Cassidy, E.N. Gary, J. Love, M. C. Franklin, J.J. Height, Structures of human acetylcholinesterase in complex with pharmacologically important ligands, *J. Med. Chem.* 55 (22) (2012) 10282–10286.
- [46] T.L. Rosenberry, X. Brazzolotto, I.R. Macdonald, M. Wandhammer, M. Trovaslet-Leroy, S. Darvesh, F. Nachon, Comparison of the binding of reversible inhibitors to human butyrylcholinesterase and acetylcholinesterase: a crystallographic, kinetic and calorimetric study, *Molecules* 22 (12) (2017) E2098.